

Polyester-Based Polyelectrolyte Complexes: Combining Thermo- and Saloplastic Properties

Julian Engelhardt, Han Zuilhof, Jasper van der Gucht, Louis C.P.M. de Smet,* and Evelien Maaskant*

Cite This: *ACS Appl. Polym. Mater.* 2024, 6, 4409–4418

Read Online

ACCESS |

Metrics & More

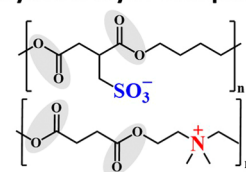
Article Recommendations

Supporting Information

ABSTRACT: In this work, we describe the synthesis of polyester-based polyelectrolytes and their corresponding polyelectrolyte complexes (PECs). The polyelectrolytes were prepared via melt polycondensation from partially biobased building blocks. Subsequently, these polyelectrolytes were combined to form polyester PECs (P-PECs) or hybrid complexes (H-PECs) by combining polyester- and vinyl-based polyelectrolytes. The complexation behavior and the thermo-mechanical properties of P-PEC and H-PECs were compared with PECs exclusively made from vinyl-based polyelectrolytes (V-PECs). Dynamic mechanical analysis (DMA) and differential scanning calorimetry (DSC) reveal a glass-transition temperature of approximately 50 °C for P-PEC. Additionally, the stability of PECs in 0.6 M NaCl was assessed, demonstrating the dissolution of P-PEC within 30 min. Neither H-PECs nor V-PECs showed dissolution after 31 days and did not exhibit any indication of a temperature-triggered phase transition. Increasing the relative humidity enhances the strain at the break of all complexes. Overall, P-PECs exhibit, in the dry state, a unique combination of saloplastic and thermoplastic properties.

KEYWORDS: polyester, polyelectrolyte complex, melt polycondensation, glass transition, saloplastic

Polyester-based Polyelectrolyte Complex

 $T_g \sim 50^\circ\text{C}$

without plasticizer



1. INTRODUCTION

Polyelectrolytes (PEs) are macromolecules with charged repeating units. They are abundant in nature and reach from basic proteins such as histones in eukaryotic cell nuclei,¹ to polysaccharides like alginic acid, a skeletal component of seaweed.² Adapting from nature, synthetic polyelectrolytes have been fabricated to mimic and improve upon such functions for various applications such as superabsorbers in diapers, tissue engineering, or adhesives,^{3–5} and have as the advantage that they allow control over the charge density, molecular weight, chemical, mechanical, and thermal stability. Mixing aqueous solutions of oppositely charged polyelectrolytes results in the formation of polyelectrolyte complexes (PECs), which are connected by intermolecular ionic cross-links.⁶ Depending on the polymeric backbone, the chemical nature of the charged groups, and the salt concentration, soft coacervates or solid aggregates can be obtained.⁷ As a result of these strong ionic cross-links, PECs are mainly studied under hydrated conditions,⁸ where water and salt are required to plasticize the ionic groups, a property known as saloplasticity.⁹ However, PECs tend to become brittle and unprocessable under poorly hydrated or dry conditions due to their strong ionic cross-links.^{6,9,10} The processing of PECs remains challenging without plasticization, primarily because of thermally induced degradation before reaching a glass transition temperature. This limits their applicability in the field of engineering materials.^{11,12} Additionally, common synthetic PEs consist of fossil-based vinyl building blocks

consisting of a C–C backbone and lack the implementation of sustainable and renewable resources.^{13–15} As of now, the design of PECs that combine thermoplastic and saloplastic properties under dry conditions, while overcoming their inherent brittleness, has not been addressed. One of the key parameters to achieve this would involve decreasing the charge density by balancing the charges in the polymeric backbone and touching upon the interface between saloplastic and thermoplastic properties.

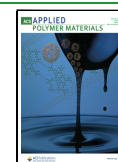
In this work, we report the synthesis of partially biobased polyelectrolytes with flexible backbones and controlled charge density to reduce the brittleness of PECs and improve their sustainability by the incorporation of a hydrolyzable polyester backbone.¹⁶ All polyesters were prepared via industrially relevant melt polycondensation. Subsequently, these polyelectrolytes were employed to prepare polyester-based polyelectrolyte complexes (P-PECs). Additionally, hybrid complexes (H-PECs) containing one vinyl-based polyelectrolyte and one polyester-based polyelectrolyte were also prepared. Furthermore, the complexation behavior and mechanical properties of

Received: October 24, 2023

Revised: March 28, 2024

Accepted: March 29, 2024

Published: April 11, 2024



P-PECs and H-PECs were compared to those of vinyl-based PECs (V-PECs).

2. EXPERIMENTAL SECTION

2.1. Chemicals and Materials. Dimethyl succinate (99%), iodomethane (99%, stabilized), itaconic acid (99+%), sodium bisulfite (ACS reagent), and titanium(IV) isopropoxide ($\text{Ti}(\text{OiPr})_4$, 98+%) were obtained from Acros Organics, *N*-methyl diethanolamine (MDEA, $\geq 99\%$), spectra/por6 (1 kDa), *p*-xylene (anhydrous), sodium polystyrenesulfonate (PSS, 70 kDa), PSS 10 kDa (narrow standard), and polydiallyldimethylammonium chloride (PDADMAC, 200–350k M_w) were obtained from Sigma-Aldrich, potassium trifluoroacetate (98%) was purchased from Fisher Scientific, tetrahydrofuran (THF, stabilized) and methanol (MeOH, absolute) were obtained from Biosolve, MeOH (anhydrous) was obtained from Macron fine chemicals, 1,1,1,3,3,3-hexafluor-2-propanol (HFIP, 99%) was obtained from Fluorochem, butanediol ($>99\%$) was obtained from TCI Europe, sodium chloride (NaCl $> 99.5\%$) was obtained from J.T. Baker. Two samples of PSS (one with 50% charge density and 30–50 kDa and another one with 100% charge density and 15–30 kDa) were obtained from Tosoh Europe B.V. All experiments were performed with Milli-Q water (18 m Ω) unless stated differently. All chemicals were used as received.

2.2. Synthesis. **2.2.1. Dimethyl Sodium Sulfo Methyl Succinate.** **2.2.1.1. Step 1: Sodium Sulfo-Itaconic Acid.** The synthesis of sodium sulfo methyl succinate was adapted from the literature.¹⁷ A 250 mL three-necked round-bottom flask equipped with a magnetic stirring bar and a reflux condenser was charged with sodium bisulfite (20.80 g, 0.20 mol) and deionized water (100 mL). After complete dissolution, itaconic acid (28.60 g, 0.22 mol) was slowly added in several portions. The mixture was heated to 90 °C under a continuous flow of nitrogen gas for 6 h. The resulting homogeneous mixture was allowed to cool to room temperature. Subsequently, 15 mL of hydrochloric acid (0.1 M) was added to the mixture, and stirring was continued for 1 h. The solvent was then evaporated under reduced pressure, resulting in the collection of a white solid product, which was further dried in a vacuum oven at 50 °C overnight. The obtained white powder was finally washed 5 times with 30 mL of ethanol to remove the excess of itaconic acid and residual impurities. The crude product was again dried in the vacuum oven at 50 °C for 24 h, yielding 43.09 g (92%) of analytically pure sodium sulfo-itaconic acid as a white powder.

¹H NMR (400 MHz, D_2O) δ 3.41 (dd, $J = 13.9, 5.7$ Hz, 1H), 3.30–3.22 (m, 1H), 3.18 (dd, $J = 13.9, 6.9$ Hz, 1H), 2.95–2.82 (m, 2H).

2.2.1.2. Step 2: Dimethyl Sodium Sulfo Methyl Succinate. A 500 mL three-necked round-bottom flask, equipped with a magnetic stirring bar and a reflux condenser, was charged with SSIA (15.0 g, 64.1 mmol), methanol (200 mL), and sulfuric acid (15 drops). The white cloudy solution was stirred under reflux at 85 °C under a continuous flow of nitrogen gas for 8 h and then cooled to room temperature. The solution was filtered to remove any unreacted SSIA. The filtrate was evaporated under reduced pressure (30 mbar) on a rotary evaporator, yielding a white crystalline solid. The crude product was recrystallized in methanol and then washed thoroughly several times with 150 mL of petroleum ether, followed by 100 mL of acetone. The pH was monitored with pH paper to ensure the complete removal of sulfuric acid. After removing all the solvents by vacuum filtration, the white powder was dried under vacuum at 50 °C for 12 h yielding 15.3 g (91%) of analytically pure dimethyl sodium sulfo methyl succinate.

¹H NMR (400 MHz, D_2O): δ 3.77 (s, 3H), 3.74 (s, 3H), 3.40–3.31 (m, 2H), 3.25–3.17 (m, 1H), 2.92 (t, $J = 6.8$ Hz, 2H).

2.2.2. Polyanion (PI). Polycondensation reaction was conducted in 100 mL three-neck round-bottom flasks equipped with a mechanical overhead stirrer (Büchi, bmd 075), an inlet for gaseous nitrogen, and a Liebig condenser. In a typical polymerization dimethyl sodium sulfo methylsuccinate (15.00 g, 81.4 mmol) and 1.3 equiv of butanediol were charged into the reaction flask. The setup was placed under a vacuum and purged with nitrogen gas, and this cycle was repeated five

times. The polycondensation method involved two stages. During the first stage, the reaction was carried out under gaseous nitrogen to form the oligomers. The reaction mixture was heated in a DrySyn at 120–140 °C for 20 min under constant stirring. After observing the complete melt of the mixture, $\text{Ti}(\text{OiPr})_4$ in *p*-xylene (0.2 g/mL) was added to the flask under a continuous flow of nitrogen. The temperature was then increased to 180 °C, and the mixture was stirred for 2 h. The temperature was then gradually increased to 200 °C with 10 °C/h, and the mixture was stirred for 2 h, as methanol and *p*-xylene were obtained in the collection flask. In the second stage of the polycondensation, the vacuum was gradually applied (reaching 0.02 mbar) after 1 h and the temperature was increased with 10 °C/h to 220 °C. Finally, the mixture was cooled down to room temperature under a nitrogen atmosphere. The reaction flask was immersed in liquid nitrogen, and the polymer was crushed with a spatula and obtained as a brittle light brown powder (14.67 g, 50.9 mmol) with a 63% yield. The crude polymer (~ 7.5 g) was dissolved in 60 mL of Milli-Q water and loaded in a Spectrapore dialysis tube with a 1 kDa cutoff. The sealed tube was immersed in a 2 L cylinder filled with Milli-Q water, which was exchanged twice a day. After 3 days, the content of the tube was recovered and concentrated by a rotary evaporator, yielding 3.8 g of transparent brown glassy polyester I with 50% yield.

¹H NMR (400 MHz, D_2O) δ 4.40 (d, $J = 7.0$ Hz, 4H), 3.64–3.49 (m, 2H), 3.49–3.34 (m, 1H), 3.14 (q, $J = 5.4$ Hz, 2H), 2.04–1.88 (m, 4H).

2.2.3. Polycation (PII). **2.2.3.1. Step 1: Polymerization.** Polycondensation reaction was conducted in 100 mL three-neck round-bottom flasks equipped with a mechanical overhead stirrer, an inlet for gaseous nitrogen, and a Liebig condenser. Dimethyl succinate (20.02 g, 0.137 mol) and methyl diethanolamine (20.40 g, 0.171 mol) were charged into the reaction flask. The setup was placed under vacuum and purged with nitrogen gas, and this cycle was repeated five times. The polycondensation method involves two stages. During the first stage, the reaction was carried out under gaseous nitrogen to form oligomers. The reaction mixture was heated in DrySyn at 160 °C for 10 min with constant stirring. Subsequently, $\text{Ti}(\text{OiPr})_4$ was added to the flask under a continuous flow of nitrogen. The temperature was then gradually increased with 10 °C/h, and the mixture was stirred for 3 h, as methanol was received in the collection flask. In the second stage of the polycondensation, the vacuum was gradually applied (reaching 0.02 mbar) after 1 h and the temperature was increased from 10 °C/h to 240 °C. The reaction was continued for 2 h, and the mixture was cooled to room temperature under a nitrogen atmosphere. Polyester IIa was obtained dark brown/black highly viscous, and hygroscopic material was obtained (26.0 g, 0.129 mol) with 94% yield.

PIIa: ¹H NMR (400 MHz, DMSO) δ 4.07 (t, $J = 5.9$ Hz, 4H), 2.61 (t, $J = 5.9$ Hz, 4H), 2.54 (s, 4H), and 2.23 (d, $J = 9.3$ Hz, 3H).

2.2.3.2. Step 2: Alkylation with Iodomethane. Polyester IIa (22.0 g, 99.4 mmol) was dissolved in 200 mL of THF. Subsequently, 3 equiv of iodomethane (MeI) was slowly added under stirring. After 20 min, the product precipitated as a light brown, spongy solid. The polymer was washed thoroughly with THF and dried in the vacuum oven at 50 °C for 48 h yielding 34.1 g of PIIb in quantitative yield.

PIIb: ¹H NMR (400 MHz, D_2O) δ 4.59 (d, $J = 6.6$ Hz, 4H), 3.82 (d, $J = 5.8$ Hz, 4H), 3.27–3.20 (m, 6H), 2.78–2.71 (m, 4H).

2.2.3.3. Step 3: Dialysis and Ion-Exchange. PIIb (9.1 g, 26.5 mmol) was dissolved in 200 mL of Milli-Q water and loaded in a Spectrapore dialysis tube with a 1 kDa cutoff. The sealed tube was immersed in a 2 L cylinder filled with a 0.3 M NaCl solution. The dialysate was exchanged twice a day. After 2 days, the water was exchanged for DWI water. After 2 days, the content of the tube was recovered and filtered through a 0.2 μm aerodisc filter. Subsequent evaporation and drying in the vacuum oven yielded a tough brown solid PIIc (4.1 g, 16.4 mmol) with 62% yield.

PIIc: ¹H NMR (400 MHz, D_2O _salt) δ 4.99–4.86 (m, 4H), 4.25–4.13 (m, 4H), 3.62–3.53 (m, 6H), 3.15–2.98 (m, 4H).

2.3. PEC Preparation. **2.3.1. Complexation.** The complexation procedure was adapted from the literature.^{18–20} The polyelectrolytes

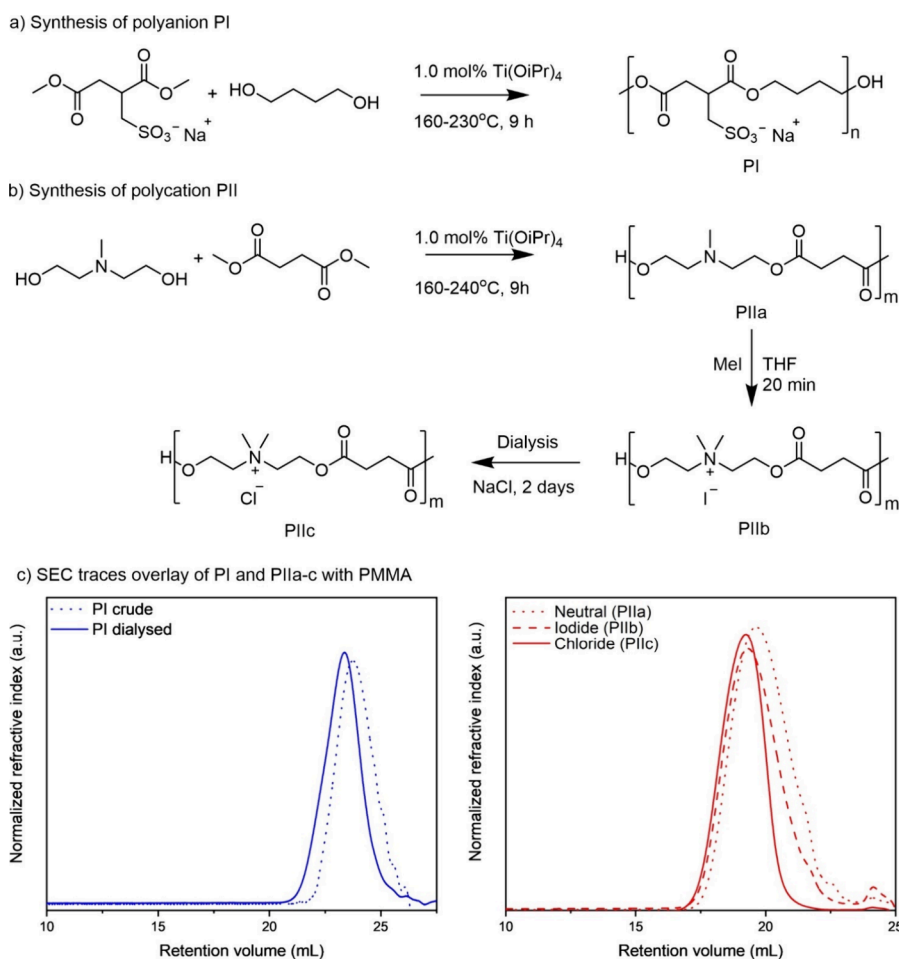


Figure 1. (a) Synthesis of polyanion PI. (b) Synthesis of polycation PII and (c) examples of the normalized refractive index (RI) signals obtained with size-exclusion chromatography for PI and PIIa–c.

were dried for 24 h in a vacuum oven prior to complexation. Molar solutions (125/250 mM) according to their repeating units were obtained by mixing the polyelectrolytes with Milli-Q water. P-PEC and H-PEC complexes were obtained without the addition of salt during the complexation process. The complexation for V-PEC was performed in 250 mM KBr. Stoichiometric amounts of the dissolved polyelectrolytes were simultaneously mixed in a beaker and stirred for 30 min. The complexation occurred instantly. After the stirring was stopped, a two-phase system was obtained. The decant was removed, and the complex was washed 3 times with Milli-Q water. An overview of the complexation, including photographs and the calculated yield of complexation is given in the Supporting Information (Table S2).

2.3.2. Hot Pressing. The processing conditions were adapted from the literature.¹⁹ Hydrated polyelectrolyte complexes were dried on a glass fiber-reinforced Teflon sheet ($\sim 120 \mu\text{m}$) on a hot plate at 80°C for 3 min. The rubbery complex was transferred into a $20 \times 5 \times 0.2 \text{ mm}^3$ aluminum mold. The complexes were pressed with a PHI 75 ton hydraulic press for 5 min (polyester-based) or 10 min (hybrid and vinyl-based) at 5 kilotons. The hot press was allowed to cool to room temperature before removing the complex from the mold. Tensile bars (specimen length 35 mm, thickness 0.2 mm, gage width 2 mm) were prepared by the same procedure. The processed complexes were stored in a desiccator at room temperature. Different relative humidities were created by a concentrated salt solution of potassium acetate (23%), by a controlled relative humidity chamber (50%), and by anhydrous magnesium sulfate under vacuum in a desiccator (0%).²¹ The processed complexes were equilibrated at 20°C for 1 week.

2.4. Characterization. Melting point measurements were conducted on a Mettler Toledo MP80 instrument. Melting points

were automatically detected and recorded when 40% of the material was molten. To this end, the samples were tightly packed in a melting point capillary, and all measurements were performed with a heating rate of $10.0^\circ\text{C}/\text{min}$.

NMR measurements were conducted on a 400 MHz Bruker Advance III at 298 K, and the resulting data were analyzed using MestReNova software, version 14.1.0–24037. Chemical shifts were derived in parts per million (ppm). Measurements in DMSO- d_6 were calibrated at DMSO peaks at 2.50 ppm for ^1H spectra, and 39.52 ppm for ^{13}C spectra, and for spectra measured in D_2O , the calibration was performed with the D_2O peaks at 4.79 ppm (1H spectra). Abbreviations used in the description of NMR data are as follows: chemical shift ($\delta = \text{ppm}$), multiplicity ($s = \text{singlet}$, $d = \text{doublet}$, $t = \text{triplet}$, $q = \text{quartet}$, $p = \text{pentet}$, $s = \text{sextet}$, $h = \text{heptet}$, $dt = \text{doublet of triplets}$, $m = \text{multiplet}$, $br = \text{broadened}$), and coupling constant (J , Hz). The PECs were dissolved according to the literature for measuring their stoichiometric composition.⁵ Around 30 mg of the dried complex were dissolved in 1 mL of 2.5 M KBr in D_2O . The ^{13}C NMR spectra were measured with concentrations of $\sim 37 \text{ mg/mL}$, with 2048 scans, and 1 s relaxation delay.

XPS measurements were performed by using a JPS-9200 photoelectron spectrometer (JEOL Ltd., Japan). All samples were analyzed using a focused monochromated Al $K\alpha$ X-ray source (spot size of $300 \mu\text{m}$) at a constant dwelling time for a survey scan of 50 ms and narrow scan of 100 ms and pass energy: survey scan = 50 eV and narrow scan = 10 eV. The power of the X-ray source was 240 W (20 mA and 12 kV). Charge compensation was applied during the XPS scans with an accelerating voltage of 2.8 eV and a filament current of 4.8 A. XPS survey-scan and narrow-scan spectra were obtained under ultrahigh vacuum conditions (base pressure = $3 \times 10^{-7} \text{ Pa}$). All

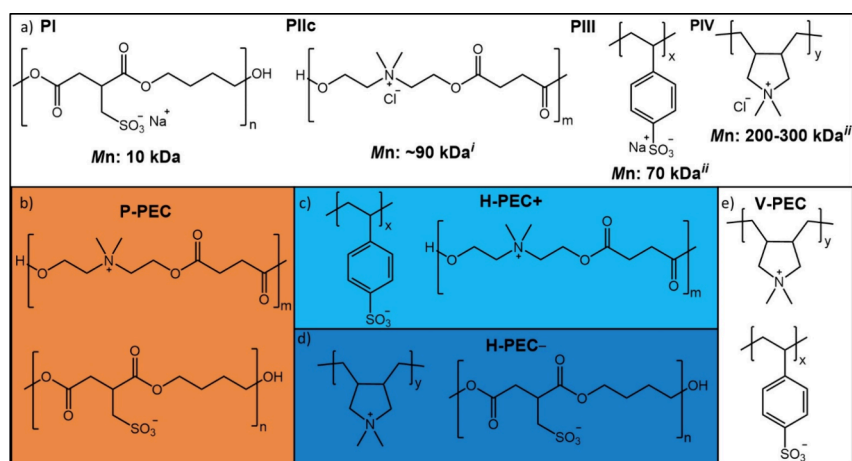


Figure 2. Chemical structures of (a) the polyanion (PI) and the polycation (PIIc), and the commercial vinyl-based polymers PSS (PIII) and PDADMAC (PIV) with their respective molecular weights and poly dispersities (ⁱFurther details on the M_n calculation of PIIc can be found in the Supporting Information. ⁱⁱThe polydispersity of commercial samples has not been measured). The combinations of oppositely charged polyelectrolytes result in the formation of different complexes: (b) P-PEC (polyester-based PI and PIIc), (c) H-PEC- (hybrid- PI and PIV), (d) H-PEC+ (hybrid+ PIII and PIIc), and (e) V-PEC (vinyl-based PIII and PIV).

narrow-range spectra were corrected with a linear background before fitting. The spectra were fitted with symmetrical Gaussian/Lorentzian (GL (30)) line shapes using CasaXPS. All spectra were referenced to the C 1s peak attributed to C–C and C–H atoms at 285.0 eV. The broad scan was measured from 0 to 1100 eV binding energy.

The molecular weights of the neutral and the cationic polyesters were determined on an Omnisec HP-SEC system equipped with a triple detector array (right-angle light scattering (RALS), low-angle light scattering (LALS), and refractive index (RI) detector and viscometer) on HFIP (model CHR6000 sn. MAL 1202615) equipped with two \times SEC columns (PSS, PFG, analytical, linear M), and a guard column, molecular range of $250\text{--}2.5 \times 10^6$ D (PMMA in HFIP). Data were calculated with OmniSEC software (version 11.32) assuming 100% mass recovery with the dn/dc values obtained from the individual sample concentrations. Hexafluoroisopropanol (HFIP) containing 0.02 M potassium trifluoroacetate was used as the eluent with a 100 μ L injection volume and a flow rate of 0.7 mL/min. Samples at concentrations of 15–30 mg/mL were dissolved overnight and filtered over a 0.45 μ m PTFE filter before injection. Narrow standard PolyCal PMMA 50 kDa (from Viscotek) was used for absolute calibration of the system ($M_w = 51.550$, $DPI = 1.024$, $W_t = 21.14$ mg/10 mL eluent).

The molecular weight of the anionic polyesters was determined on a Viscotek VE2001 GPCmax equipped with a TDA305 triple detector array (right-angle light scattering (RALS), low-angle light scattering (LALS), and refractive index (RI) detector and viscometer) and a 3 \times SEC column (Ultrasphere) with a molecular range of $\sim 100\text{--}4.0 \times 10^5$ D. Molecular weight data were calculated with OmniSEC software (version 5.12). Milli-Q water containing 0.1 M of sodium chloride and 0.02 M of monosodium phosphate was used as the eluent with a flow rate of 0.7 mL/min. Samples (10–20 mg/mL) were dissolved overnight and filtered over 0.45 μ m cellulose acetate syringe filters before injection. The system was calibrated with a narrow PSS standard from Merck (~ 30 kg/mol).

The thermal stability of the polyesters was determined by using a PerkinElmer STA6000 by heating the samples (1–5 g) from room temperature to 400/700 $^{\circ}$ C at 10 $^{\circ}$ C/min under a continuous flow of nitrogen gas or air (20 mL/min).

A Q800 instrument from TA Instruments equipped with film clapping was used for extensional oscillatory measurements. An amplitude sweep was performed at room temperature and at 1 Hz to determine the linear viscoelastic regime. Subsequently, temperature sweeps were performed between 25 $^{\circ}$ C and 150 $^{\circ}$ C with 3 $^{\circ}$ C/min with 0.03% strain and at 1 Hz under a constant flow of nitrogen.

Tensile tests were performed on the aforementioned Q800 and at different relative humidities at room temperature. The samples were clamped and subjected to a linear stress ramp of 3 N/min until they broke. The humidity is controlled by a humidifier to 23 and 50% throughout the whole measurements.

Zeta potential measurements were performed on a ZS-Nano (Malvern) equipped with a 632.8 nm HeNe laser and APD detector. 0.3 mL of polymer solution of 250 mM according to their repeating unit were measured in 10×10 mm² plastic cuvette at 25 $^{\circ}$ C.

Differential scanning calorimetry (DSC) measurements were performed using a PerkinElmer DSC 8000 instrument provided with liquid nitrogen cooling and an autosampler. Stainless steel DSC cups with a rubber O-ring were used. The following protocol was used: two scans from -70 to 150 $^{\circ}$ C with a heating with 10 min isothermal steps at the limits and cooling rate of 10 $^{\circ}$ C/min.

3. RESULTS AND DISCUSSION

The anionic polyester (PI) was synthesized directly via melt polycondensation of a sulfonated dimethyl ester and a non-charged diol, while the cationic polyester (PIIc) was obtained via melt polycondensation of two non-charged monomers, followed by subsequent postmodification as shown in Figure 1. The structures of the synthesized polymers were confirmed using ¹H NMR (Figures S7–S11) and ¹³C NMR spectroscopy (Figures S23 and S24). The molecular weights of the polyelectrolytes were estimated using triple detection size exclusion chromatography (SEC), giving an M_n of 10 kDa for PI. The M_n values of polymers PIIa and PIIb were found to be approximately 90 kDa. Note that the SEC system used to characterize PIIa-c was devised for non-charged polymers, as injection of PIIa-c on the aqueous SEC system used for the characterization of PI did not result in any detector signal. Surprisingly, the M_n for PIIc, after ion exchange and dialysis, was found to be significantly higher (164 kDa). A minor increase in molecular weight can be explained by the removal of low molecular weight species, which is indeed observed in the SEC detector signals (Figures 1c and S2–S4). However, the found increase is significantly larger than what can be expected as the molecular weight cutoff of the dialysis tube was 1 kDa. Furthermore, the polydispersity (\mathcal{D}) for polymers PIIa–PIIc was found to be 1.2–1.3 which is far below the expected value of 2 for polycondensation polymers. Thus, it can be

Table 1. Summary of the Complex Composition and Properties

| Complex | Phase Separation | Appearance ^a | Yield ^b (wt %) | XPS S/N ratio | ¹ H- NMR anion /cation | T _g (°C) DSC/ DMA |
|---------|---------------------|---|------------------------------|------------------|--|------------------------------------|
| P-PEC | Liquid-liquid |  | 39 | 0.9 | 1.16 _c | ~50/52 |
| H-PEC- | Liquid-solid |  | 62 | 1.0 | 0.98 | ^d |
| H-PEC+ | Liquid-solid |  | 73 | 0.9 | 0.75 ^e | ^d |
| V-PEC | Liquid-solid |  | 90 | 0.8 | 1.12 | ^d |

^aAll samples appeared to be homogeneous and transparent after hot pressing. ^bMaximum relative yield of polymer without counterions or salts. ^cRatio was calculated by comparing the integral of isolated peaks of PI and PIIC via ¹H NMR. ^dNo T_g was observed. ^eH-PEC+ did not completely dissolve.

concluded that the SEC system was not fully suited for the characterization of the cationic polymers. A more in-depth discussion on the SEC results is given in the [Supporting Information](#). Unfortunately, molecular weight determination via end-group analysis was not possible due to the relatively high molecular weight and overlapping signals.

The synthesized, polyester-based, and commercial, vinyl-based PEs were used to prepare the corresponding PECs in a 1:1 stoichiometry in terms of their charged repeating units ([Figure 2](#)).^{19,22,23} Thus, four PECs were obtained, namely: P-PEC (polyester-based PI and PIIC), H-PEC- (hybrid, PI, and PIV), H-PEC+ (hybrid, PIIC, and PIII), and V-PEC (vinyl-based, PIII and PIV). Upon mixing two aqueous PE solutions the complexation occurred instantaneously and was observed as macroscopic phase separation ([Table S2](#)). The complexation of PI and PIIC into P-PEC was further confirmed via zeta potential measurements ([Table S4](#)). Complexation into P-PEC occurred via coacervation, i.e., liquid-liquid phase separation while vinyl-containing PECs (H-PECs and V-PECs) were formed through liquid-solid phase separation. The isolated yield of complexation was 62% for H-PEC-, 73% for H-PEC+, 90% for V-PEC, and 39% for P-PEC. The difference in complexation yield may be attributed to differences in molecular weight, charge density, and the structures of the polyester-based PEs compared to those of the vinyl-based PEC.^{3,24,25} In addition, since P-PEC was obtained as a coacervate, the washing steps might have removed polyelectrolytes from the complex, resulting in a lower yield.²⁶ Notably, Li et al. investigated the effect of increasing molecular weight on polypeptide systems showing an eminent increase in complexation yield upon going from 20-mers to 50-mers, while a further increase in the molecular weight did not contribute to significantly higher yields.²⁵ While it is unknown whether polyesters show a similar trend in this regard, we do remark that the molecular weight of PI corresponds to a ~35-mer, which may explain the lower complexation yield, while the higher yield in the vinyl-based system can be attributed to the molecular weight of the corresponding PEs.²⁰ V-PEC was obtained at a yield as high as 90%, but it required the addition of salt to promote the complexation.²⁷ Without the addition of

salt (250 mM KBr), no complexation occurred for PSS/PDADMAC, which was also reported by Krishna et al. By contrast, P-PEC and H-PEC complexes were formed without the addition of salt. Interestingly, the addition of salt during P-PEC formation resulted in poorer complexation, to the point where no phase separation was observed, which is known as the critical salt concentration ([Table S2](#)).¹⁶ The salt sensitivity of P-PEC could be potentially caused by their lower charge density and molecular weight compared to their vinyl analogs.^{26,28–30}

The composition and stoichiometry of the four complexes were investigated by X-ray photoelectron spectroscopy (XPS) and ¹H NMR, showing for both techniques a (close-to-perfect) 1:1 ratio. Overall, no peaks of the respective counterions Na⁺ and Cl⁻, and in the case of V-PEC, no K⁺, and Br⁻ could be observed in the XPS spectra ([Table S3](#)). This suggests that most counterions have been removed after the washing step or taking the detection limit and general aspects of quantification via XPS into account are below the detection limit.³¹ Analysis of the N_{1s} and S_{1s} peaks allowed quantification of the ratio of the polyelectrolytes in the complex, yielding values of 0.8 to 1.0 ([Table 1](#)). Further insights into the composition of the PECs were obtained by ¹H NMR. [Figure 3](#) shows an example of the ¹H NMR spectrum obtained for P-PEC and its individual polyelectrolytes PI and PIIC. All other NMR spectra of the complexes are given in the [Supporting Information \(Figures S20–S23\)](#).

To this end, the complexes were dissolved in 2.5 M KBr in D₂O and analyzed according to the approach described by Shamoun et al.³² Except for H-PEC+, which formed a cloudy coacervate suspension, all complexes readily dissolved within a few minutes. The composition of each complex could be quantified by the integration of isolated peaks of the individual polyelectrolytes.³³ A deviation from a 1:1 stoichiometry of the complex was obtained up to 16 mol % for P-PEC. H-PEC+ showed a larger deviation with 25 mol %, which could be explained by its poor solubility. The quantitative XPS and NMR results are consistent with each other for H-PEC-. In the other cases, either XPS (surface sensitive) or NMR (bulk) indicates an excess of one of the polyelectrolytes. Ma et al.

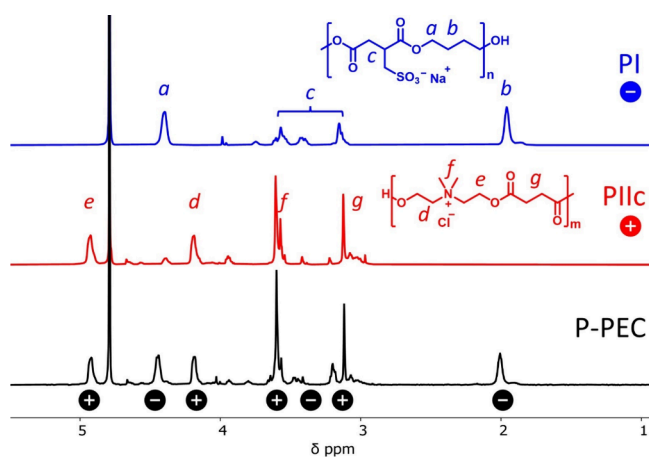


Figure 3. Overlay ^1H NMR spectra of PI (top, blue), PIIC (middle, red), and P-PEC (bottom, black) measured in 2.5 M KBr in D_2O . The proton signals of the individual polymers are assigned for PI (a–c) and PIIC (e,d,f,g). The corresponding signals of the polyelectrolytes within the complex (P-PEC) are assigned with (–) and (+) symbols in the black circles.

observed unbalanced partitioning of 1:1 stoichiometric PSS/PDADMAC systems for different salt concentrations and suggested different solubility parameters for the individual polyelectrolytes, resulting in diverging stoichiometries in the complexes.³⁴ Such effects could also influence the partitioning of the polyester-based polyelectrolytes and cause deviation from a 1:1 stoichiometry. Further research is required to learn what effects cause this deviation.

Specimens for mechanical testing of the complexes were prepared via a hot-pressing process, adapted from Krishna et al.²⁷ First, the complexes were dried on the heating plate of a

hot press for around 5 min. Subsequently, the rubbery complexes were subjected to hot-pressing by applying 5 kilotons of pressure at 80 °C for either 5 min (P-PEC) or 10 min (H-PECs and V-PEC). The longer hot-pressing times were necessary to achieve homogeneous samples for the H-PECs and V-PECs. Remarkably, only the P-PEC complexes could be processed in a dry state, after drying in the vacuum oven, whereas H-PECs and V-PECs required the presence of water as a plasticizer (Figure S58f). The processability of PECs in the dry state has also been investigated by van Lange et al., who screened the charge of the ionic groups in the polymer backbone.³⁵ This, as well as our current approach, i.e., reducing the charge density, results in PEs with thermoplastic behavior and enables the processing of the PECs even under dry and nonplasticized conditions. The complexes were obtained as homogeneously transparent materials after hot-pressing, indicating a dense structure without internal voids (Table 1).^{23,27,32}

The thermo-mechanical properties of the complexes were evaluated via dynamic mechanical analysis (DMA) by subjecting them to oscillatory deformation in a temperature ramp, ranging from ~30 to 150 °C. Prior to testing, all complexes were dried in a desiccator at 0% relative humidity (RH) for 1 week to prevent water-induced plasticization. The dryness of these samples was confirmed via TGA measurements (Table S5). The measured storage modulus, loss modulus, and loss tangent ($\tan \delta$) are presented in Figure 4. At room temperature, all complexes exhibited storage moduli within the range of 800–1800 MPa. Both H-PECs and V-PEC demonstrated storage and loss moduli that depended not strongly on the temperature, indicating the absence of phase transitions. By contrast, the storage modulus of P-PEC remained constant up to 40 °C, and then experienced a gradual decrease, reaching 100 MPa at 80 °C. Furthermore, a

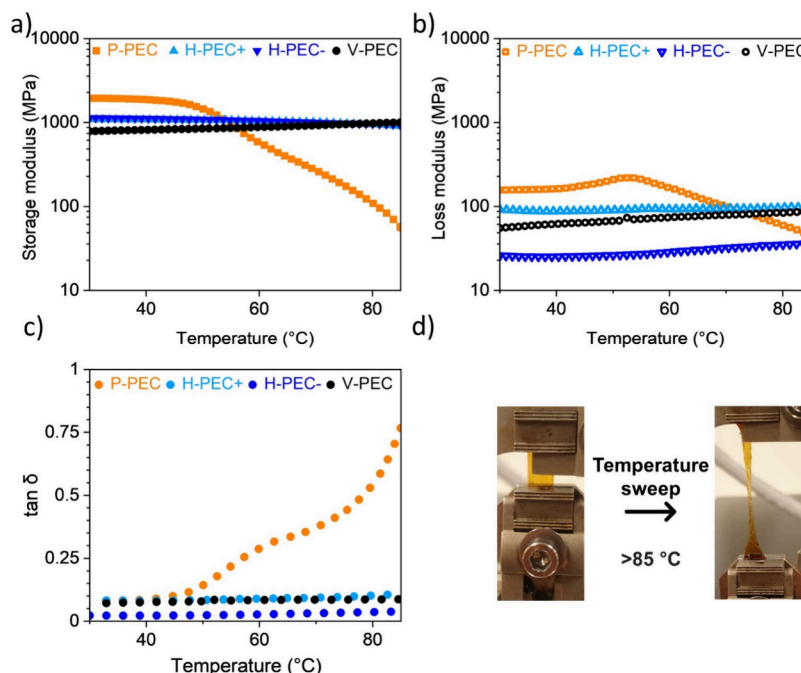


Figure 4. Temperature sweeps ranging from 30 to 85 °C were conducted on the processed complexes, showing the compiled storage (a) and loss (b) moduli, and the respective $\tan \sigma$ (c) up to 85 °C. Images of the P-PEC specimen before and after the temperature sweep are provided in panel (d), illustrating the observed thermal-induced plastic deformation. Note: Due to the plastic deformation of P-PEC the obtained data above 85 °C were not reliable; the complete data set can be found in the SI (Figure S53).

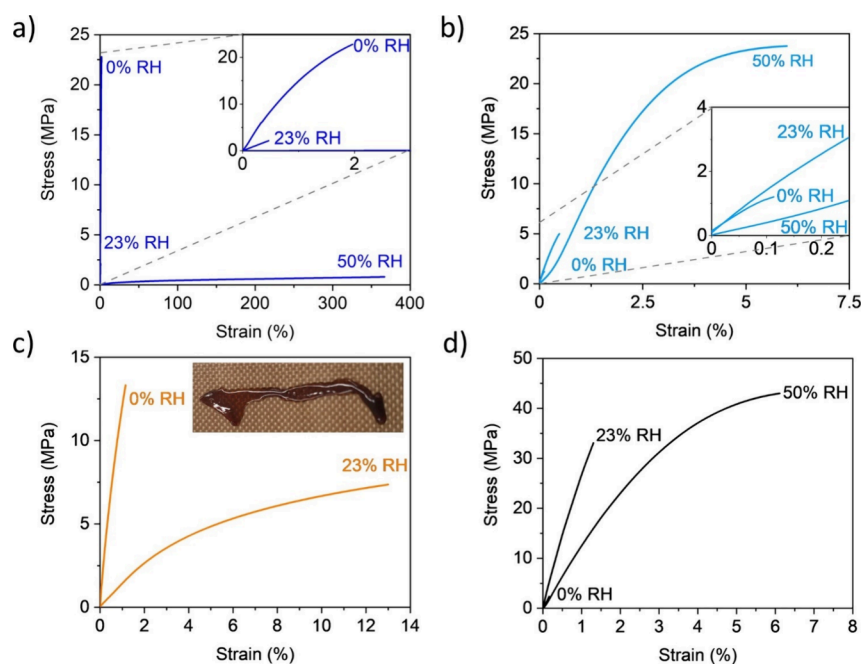


Figure 5. Representative graphs of tensile tests conducted at different RH (0, 23, and 50%) at room temperature for the complexes (a) H-PEC⁻; (b) H-PEC⁺; (c) P-PEC; at 50% RH the tensile bar was too hydrated and viscous, and it lost its shape and could not be handled properly; and (d) V-PEC.

distinct peak in the loss modulus (Figure 4b) was observed for P-PEC at 52 °C, which we attribute to the material's glass transition temperature (T_g). Neither the loss nor storage moduli showed indications of T_g for H-PECs and V-PEC. Moreover, the decrease in storage modulus was accompanied by a proportional increase in $\tan \delta$ (i.e., loss modulus divided by storage modulus; Figure 4c). This rise in $\tan \delta$ signifies a transition from an elastic-dominated response to a more viscous behavior, indicating a decrease in the material's elastic properties. Interestingly, after the temperature ramp, the P-PEC material displayed significant deformation compared to that of its initial state (Figure 4d). The material softened and displayed typical yielding without fracturing. This behavior resembles the response of a thermoplastic material above its T_g value, where segmental motion becomes possible. The ductile response observed in the material, as indicated by the deformation, suggests that even with a low applied strain (0.03%) in stress-controlled DMA, the combined effect of stress and temperature-induced plasticization is evident, as depicted by the displacement of the clamps after the measurement (Figure 4d). Notably, this thermoplastic behavior was unique to P-PEC and was not observed in the H-PECs and V-PEC. DSC measurements of the complexes were conducted to complement the DMA measurements (Figures S38–S41). H-PECs and V-PEC did not exhibit any thermal transitions up to 150 °C, which aligns with the observations from the DMA temperature sweeps. In contrast, P-PEC displayed a T_g value of approximately 50 °C, consistent with the findings from the DMA temperature sweep analysis.

Note that—to the best of our knowledge—this is the first time that the T_g of a PEC in a dry state, without the presence of plasticizing agents such as water or salt, has been measured. The combination of a lower charge density and a more flexible aliphatic backbone in the P-PEC compared to the V-PEC appears to be crucial factors contributing to this behavior.

Due to the ionic charges in the backbone, the mechanical properties of PECs can be altered by the relative humidity (RH).^{32,36} Stress–strain experiments revealed that the strain at break increased at higher RH values for all complexes, as expected (Figure 5). Except, H-PECs exhibited a higher strain at the break at 0% RH compared to 23% RH. At 50% RH, H-PEC⁺ demonstrated the lowest strain at the break with 14%, followed by V-PEC with 30%, and H-PEC⁻ with 365% (Figure S56). Although all samples were equilibrated under the same conditions, the actual water content varied among the different PEC samples. However, a clear correlation between the humidity in the equilibration chamber and the measured water content is observed (Table S6). Certain trends can be observed: (a) P-PEC is the most sensitive material to RH and could not be measured at 50% RH due to the extremely viscous and deformable nature of the specimen (Figure 5); (b) the strain shows a positive correlation with increasing RH for most samples; (c) the polymer backbone and molecular weight seem to have a strong effect on the stress and strain especially at higher RH; (d) since nonstoichiometric complexes are known to show poorer mechanical properties compared to a 1:1 ratio, the complexation of PECs could be optimized to reach their full mechanical potential.²³ At 50% RH, H-PEC⁺, and V-PEC show the highest stress values at break with 18 and 32 MPa, respectively, which can be attributed to the rigidity of PSS. Additionally, both polycations, PII and PDADMAC, have a similar and high molecular weight. In contrast, H-PEC⁻, which contains PI and PDADMAC, shows poor stress at break, with 365% elongation at break. Conversely, the lower molecular weight of PI in H-PEC⁻ and the resulting larger contribution of hydroxyl-terminated end-groups could account for its high sensitivity to RH, which is also reflected in the measured water content (Table S5). The hygroscopic properties of P-PEC can be attributed to the more hydrophilic polyester backbone of PI and PIIc, as well as the presence of their hydroxyl end groups. A large deviation in the polymer

chains would result in weaker interconnections between the PE chains, and the higher proportion of hydroxyl end-groups in PI would enhance the hydrophilic properties of P-PEC.^{23,37} This makes polyester-based PEs different from PSS and PDAD-MAC, as the latter have a hydrophobic, all-carbon backbone. The larger distribution in molecular weight, particularly for PI compared to the other polyester (PIIc), could also contribute to the moisture sensitivity of P-PEC.

The stability of the processed complexes was assessed against Milli-Q water and a 0.6 M NaCl solution, mimicking the molarity of seawater (Figure 6). A video of this stability

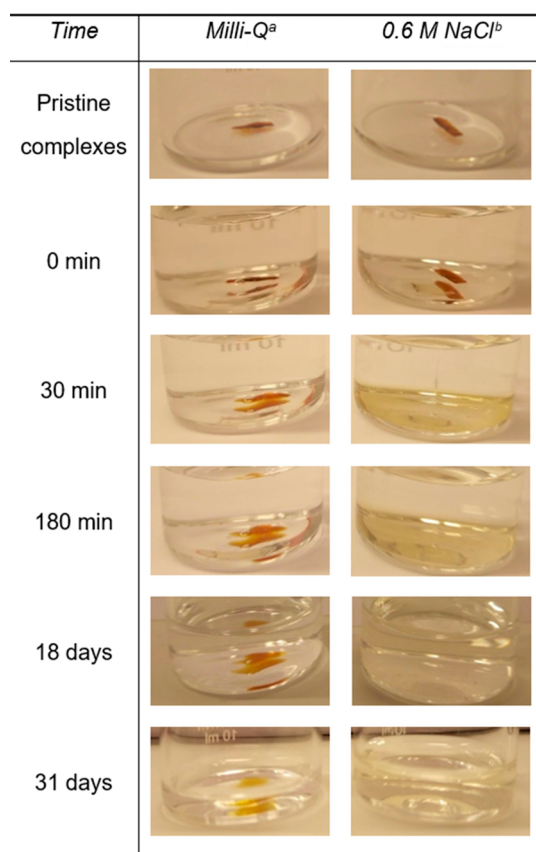


Figure 6. Pictures of the stability test of P-PEC films in (a) Milli-Q water and (b) 0.6 M NaCl solution at room temperature. The process was monitored over a period of 1 month.

test is added as Supporting Information. The P-PEC submerged in Milli-Q water showed minor swelling within the first 3 h. Even after 31 days, the complex remained intact but lost its original shape, as illustrated in Figure 6. Interestingly, after immersion in 0.6 M NaCl, the P-PEC began to dissolve instantly and was completely dissolved within 30 min. A homogeneous solution was obtained without any coacervation or phase separation visible. These results demonstrate the rapid dissolution of P-PEC in saline water. In the presence of ions, the electrostatic interactions in the P-PEC are screened, while in deionized water, only swelling of the complex is observed. By contrast, both H-PECs and V-PEC²⁴ exhibited less sensitivity to 0.6 M NaCl compared to P-PEC (Table S6). H-PECs also exhibited pronounced swelling in 0.6 M NaCl, which resulted in the formation of stable coacervate complexes. The lower charge density of the polyester-based polyelectrolytes in P-PEC suggests that fewer

ions are required to break the ionic cross-links.²⁴ Additionally, the higher flexibility and relatively shorter length of aliphatic and hydrophilic polyesters, in comparison to the bulky and more hydrophobic vinyl-based polyelectrolytes, may facilitate better water uptake within the complex and lower salt resistance.³⁷ A similar correlation between hydrophobicity and salt resistance was described by Sadman et al. for different vinyl-based complexes.³⁸ This suggests that the more hydrophilic polyester backbone could be the primary contributor to the lower salt resistance. Although there are strong indications that the water and salt sensitivity is primarily influenced by the polyester backbone and lower charge density rather than the difference in molecular weight, further investigation is necessary to fully pinpoint the origin of the observed effects.

4. CONCLUSIONS

To conclude, the polyester-based PEC displayed the desired features of quickly dissolving in 0.6 M NaCl but remaining intact in deionized water (like all PECs under the current study). Additionally, P-PEC shows a glass transition temperature of approximately 50 °C in the absence of any plasticizer. The low T_g of P-PEC allows processing in salt and water-free conditions in the dry state. Overall, the resulting P-PEC exhibits a unique combination of saloplastic and thermoplastic properties, extending the fields of both PECs and thermoplastics. To overcome the high sensitivity toward humidity, the synthesis of polyesters with a higher molecular weight and/or a more hydrophobic nature is interesting to further explore the potential of polyester-based PECs.

■ ASSOCIATED CONTENT

Supporting Information

The Supporting Information is available free of charge at <https://pubs.acs.org/doi/10.1021/acsapm.3c02566>.

¹H NMR, ¹³C NMR, and DOSY-NMR spectra, SEC traces, DMA temperature sweeps and stress–strain experiments, stability tests, and TGA and DSC measurement details (PDF)

Movie of the stability test of P-PEC (mp4)

■ AUTHOR INFORMATION

Corresponding Authors

Louis C.P.M. de Smet – Laboratory of Organic Chemistry, Wageningen University, 6708 WE Wageningen, The Netherlands; orcid.org/0000-0001-7252-4047; Email: louis.desmet@wur.nl

Evelien Maaskant – Wageningen Food & Biobased Research, 6708 WG Wageningen, The Netherlands; orcid.org/0000-0003-4691-7538; Email: evelien.maaskant@wur.nl

Authors

Julian Engelhardt – Laboratory of Organic Chemistry and Laboratory of Physical Chemistry and Soft Matter, Wageningen University, 6708 WE Wageningen, The Netherlands; Wageningen Food & Biobased Research, 6708 WG Wageningen, The Netherlands; orcid.org/0000-0003-0389-7936

Han Zuilhof – Laboratory of Organic Chemistry, Wageningen University, 6708 WE Wageningen, The Netherlands; orcid.org/0000-0001-5773-8506

Jasper van der Gucht – Laboratory of Physical Chemistry and Soft Matter, Wageningen University, 6708 WE Wageningen, The Netherlands; orcid.org/0000-0001-5525-8322

Complete contact information is available at:
<https://pubs.acs.org/10.1021/acsapm.3c02566>

Author Contributions

The manuscript was written through contributions of all authors. All authors have given approval to the final version of the manuscript.

Funding

This work was performed within the context of the strategic investment theme “Connected Circularity” of Wageningen University & Research.

Notes

The authors declare no competing financial interest.

ACKNOWLEDGMENTS

This work was supported by the Connected Circularity program within Wageningen University & Research. The authors thank Barend van Lagen, Yanzhang Lou, and Herman de Beukelaer for technical assistance and Sophie van Lange, Willem Vogelzang, and Francis Duivenvoorde for the fruitful discussions regarding material synthesis and characterization (all Wageningen University & Research).

REFERENCES

- (1) Schiessel, H. The Physics of Chromatin. *J. Phys.: Condens. Matter* **2003**, *15* (19), R699–R774.
- (2) Pereira, L. *Alginates - Recent Uses of This Natural Polymer*; Pereira, L., Ed.; IntechOpen, 2020.
- (3) Bediako, J. K.; Mouele, E. S. M.; El Ouardi, Y.; Repo, E. Saloplastics and the Polyelectrolyte Complex Continuum: Advances, Challenges and Prospects. *Chemical Engineering Journal* **2023**, *462*, No. 142322.
- (4) Mortimer, D. A. Synthetic Polyelectrolytes—A Review. *Polym. Int.* **1991**, *25* (1), 29–41.
- (5) Philipp, B.; Dautzenberg, H.; Linow, K.; Kotz, J.; Dawydoff, W. Polyelectrolyte complexes-recent developments and open problems. *Prog. Polym. Sci.* **1989**, *14*, 91–172.
- (6) Michaels, A. S. Polyelectrolyte Complexes. *Ind. Eng. Chem.* **1965**, *57* (10), 32–40.
- (7) Wang, Q.; Schlenoff, J. B. The Polyelectrolyte Complex/Coacervate Continuum. *Macromolecules* **2014**, *47* (9), 3108–3116.
- (8) Luo, F.; Sun, T. L.; Nakajima, T.; Kurokawa, T.; Zhao, Y.; Sato, K.; Ihsan, A. Bin; Li, X.; Guo, H.; Gong, J. P. Oppositely Charged Polyelectrolytes Form Tough, Self-Healing, and Rebuildable Hydrogels. *Adv. Mater.* **2015**, *27* (17), 2722–2727.
- (9) Porcel, C. H.; Schlenoff, J. B. Compact Polyelectrolyte Complexes: “Saloplastic” Candidates for Biomaterials. *Biomacromolecules* **2009**, *10* (11), 2968–2975.
- (10) Bediako, J. K.; Mouele, E. S. M.; El Ouardi, Y.; Repo, E. Saloplastics and the Polyelectrolyte Complex Continuum: Advances, Challenges and Prospects. *Chemical Engineering Journal* **2023**, *462*, No. 142322.
- (11) Chen, Y.; Yang, M.; Schlenoff, J. B. Glass Transitions in Hydrated Polyelectrolyte Complexes. *Macromolecules* **2021**, *54* (8), 3822–3831.
- (12) Schaaf, P.; Schlenoff, J. B. Saloplastics: Processing Compact Polyelectrolyte Complexes. *Adv. Mater.* **2015**, *27* (15), 2420–2432.
- (13) Basu, S.; Plucinski, A.; Catchmark, J. M. Sustainable Barrier Materials Based on Polysaccharide Polyelectrolyte Complexes. *Green Chem.* **2017**, *19* (17), 4080–4092.
- (14) Shi, R.; Sun, T. L.; Luo, F.; Nakajima, T.; Kurokawa, T.; Bin, Y. Z.; Rubinstein, M.; Gong, J. P. Elastic–Plastic Transformation of Polyelectrolyte Complex Hydrogels from Chitosan and Sodium Hyaluronate. *Macromolecules* **2018**, *51* (21), 8887–8898.
- (15) Solier, Y. N.; Mocchiutti, P.; Inalbon, M. C.; Zanuttini, M. A. Thermoplastic Films Based on Polyelectrolyte Complexes of Arabino Glucurono-Xylan and Polyethylenimine. *Macromol. Mater. Eng.* **2022**, *307* (10), No. 202200108.
- (16) Larrañaga, A.; Lizundia, E. A Review on the Thermomechanical Properties and Biodegradation Behaviour of Polyesters. *Eur. Polym. J.* **2019**, *121*, No. 109296.
- (17) Xu, J.; Cao, F.; Li, T.; Zhang, S.; Gao, C.; Wu, Y. Itaconic Acid Based Surfactants: I. Synthesis and Characterization of Sodium n-Octyl Sulfoitaconate Diester Anionic Surfactant. *J. Surfactants Deterg* **2016**, *19* (2), 373–379.
- (18) Hariiri, H. H.; Schlenoff, J. B. Saloplastic Macroporous Polyelectrolyte Complexes: Cartilage Mimics. *Macromolecules* **2010**, *43* (20), 8656–8663.
- (19) Krishna B, A.; Willott, J. D.; Lindhoud, S.; de Vos, W. M. Hot-Pressing Polyelectrolyte Complexes into Tunable Dense Saloplastics. *Polymer* **2022**, *242*, No. 124583.
- (20) Porcel, C. H.; Schlenoff, J. B. Compact Polyelectrolyte Complexes: “Saloplastic” Candidates for Biomaterials. *Biomacromolecules* **2009**, *10* (11), 2968–2975.
- (21) Engineering Toolbox; Saturated Salt Solutions and control of Air Humidity. 2014 Available at: https://www.engineeringtoolbox.com/salt-humidity-d_1887.html (accessed April 30, 2023).
- (22) Shamoun, R. F.; Reisch, A.; Schlenoff, J. B. Extruded Saloplastic Polyelectrolyte Complexes. *Adv. Funct. Mater.* **2012**, *22* (9), 1923–1931.
- (23) Chen, Y.; Yang, M.; Shaheen, S. A.; Schlenoff, J. B. Influence of Nonstoichiometry on the Viscoelastic Properties of a Polyelectrolyte Complex. *Macromolecules* **2021**, *54* (17), 7890–7899.
- (24) Neitzel, A. E.; Fang, Y. N.; Yu, B.; Rummyantsev, A. M.; de Pablo, J. J.; Tirrell, M. V. Polyelectrolyte Complex Coacervation across a Broad Range of Charge Densities. *Macromolecules* **2021**, *54* (14), 6878–6890.
- (25) Li, L.; Srivastava, S.; Andreev, M.; Marciel, A. B.; de Pablo, J. J.; Tirrell, M. V. Phase Behavior and Salt Partitioning in Polyelectrolyte Complex Coacervates. *Macromolecules* **2018**, *51* (8), 2988–2995.
- (26) Wang, Q.; Schlenoff, J. B. The Polyelectrolyte Complex/Coacervate Continuum. *Macromolecules* **2014**, *47* (9), 3108–3116.
- (27) Krishna B, A.; Lindhoud, S.; de Vos, W. M. Hot-Pressed Polyelectrolyte Complexes as Novel Alkaline Stable Monovalent-Ion Selective Anion Exchange Membranes. *J. Colloid Interface Sci.* **2021**, *593*, 11–20.
- (28) van der Gucht, J.; Spruijt, E.; Lemmers, M.; Cohen Stuart, M. A. Polyelectrolyte Complexes: Bulk Phases and Colloidal Systems. *J. Colloid Interface Sci.* **2011**, *361* (2), 407–422.
- (29) Digby, Z. A.; Yang, M.; Lteif, S.; Schlenoff, J. B. Salt Resistance as a Measure of the Strength of Polyelectrolyte Complexation. *Macromolecules* **2022**, *55* (3), 978–988.
- (30) Li, L.; Srivastava, S.; Andreev, M.; Marciel, A. B.; de Pablo, J. J.; Tirrell, M. V. Phase Behavior and Salt Partitioning in Polyelectrolyte Complex Coacervates. *Macromolecules* **2018**, *51* (8), 2988–2995.
- (31) Fares, H. M.; Ghossoub, Y. E.; Surmaitis, R. L.; Schlenoff, J. B. Toward Ion-Free Polyelectrolyte Multilayers: Cyclic Salt Annealing. *Langmuir* **2015**, *31* (21), 5787–5795.
- (32) Shamoun, R. F.; Reisch, A.; Schlenoff, J. B. Extruded Saloplastic Polyelectrolyte Complexes. *Adv. Funct. Mater.* **2012**, *22* (9), 1923–1931.
- (33) Fares, H. M.; Ghossoub, Y. E.; Surmaitis, R. L.; Schlenoff, J. B. Toward Ion-Free Polyelectrolyte Multilayers: Cyclic Salt Annealing. *Langmuir* **2015**, *31* (21), 5787–5795.
- (34) Ma, Y.; Ali, S.; Prabhu, V. M. Enhanced Concentration Fluctuations in Model Polyelectrolyte Coacervate Mixtures along a Salt Isopleth Phase Diagram. *Macromolecules* **2021**, *54* (24), 11338–11350.
- (35) van Lange, S. G. M.; te Brake, D. W.; Portale, G.; Palanisamy, A.; Sprakel, J.; van der Gucht, J. Moderated Ionic Bonding for Water-

Free Recyclable Polyelectrolyte Complex Materials. *Sci. Adv.* **2024**, *10* (2), No. eadi3606.

(36) Lyu, X.; Peterson, A. M. Humidity Tempering of Polyelectrolyte Complexes. *Macromolecules* **2018**, *51* (23), 10003–10010.

(37) Li, L.; Romyantsev, A. M.; Srivastava, S.; Meng, S.; de Pablo, J. J.; Tirrell, M. V. Effect of Solvent Quality on the Phase Behavior of Polyelectrolyte Complexes. *Macromolecules* **2021**, *54* (1), 105–114.

(38) Sadman, K.; Wang, Q.; Chen, Y.; Keshavarz, B.; Jiang, Z.; Shull, K. R. Influence of Hydrophobicity on Polyelectrolyte Complexation. *Macromolecules* **2017**, *50* (23), 9417–9426.